Investigation of Pyrene vs. Anthracene-based Oxime Esters: Role of the Excited States on Their Polymerization Initiating Abilities

Mahmoud Rahal, Hugo Bidotti, Sylvain Duval, Bernadette Graff, Tayssir Hamieh, Joumana Toufaily, Frédéric Dumur, Jacques Lalevée

Investigation of Pyrene vs. Anthracene-based Oxime Esters: Role of the Excited States on Their Polymerization Initiating Abilities

Mahmoud Rahal[a,b,c], Hugo Bidotti[d], Sylvain Duval[e], Bernadette Graff [a,b], Tayssir Hamieh[c], Joumana Toufaily[c], Frédéric Dumur[d], Jacques Lalevée*[a,b]

[a] Université de Haute-Alsace, CNRS, IS2M UMR 7361, F-68100 Mulhouse, France. jacques.lalevee@uha.fr (J.L.)

[b] Université de Strasbourg, Strasbourg, France

[c] Laboratory of Materials, Catalysis, Environment and Analytical Methods (MCEMA) and LEADDER Laboratory, Faculty of Sciences, Doctoral School of Sciences and Technology (EDST), Lebanese University, Beirut 6573-14, Lebanon.

[d] Aix Marseille Univ, CNRS, ICR UMR 7273, F-13397 Marseille, France;

[e] Université de Lille, CNRS, Centrale Lille, Univ. Artois, UMR 8181 – UCCS - Unité de Catalyse et Chimie du Solide, F-59000 Lille, France

Abstract

In this work, two series of oxime esters (OXE) based on Pyrene and Anthracene chromophores were synthesized and tested as Type I photoinitiators for the Free Radical Photopolymerization (FRP) under visible irradiation at 405 nm using light-emitting diodes (LED) as the irradiation source. Interestingly, the two series of oxime esters only differ by the nature of the substituents connected to the oxime ester functional group. As a result of this modification, the reactivity of the different compounds only depends on the rate of decomposition from their excited states as well as the reactivity of the generated radicals. Remarkably, the 18 Pyrene-based OXEs (Py-OXE) and 17 Anthracene-based OXEs (An-OXE) were never synthesized prior to this work. Pyrene and Anthracene chromophores were selected as benchmark structures reacting mainly from their first excited singlet (S_1) and triplet (T_1) states, respectively. This will allow to shed some light on the excited states responsible of the cleavage of OXEs. Therefore, originality of this study relies in the difference of the initiation ability between these two families. In fact, the results showed that Py-OXEs (0.5% w) are the most efficient systems compared to An-OXEs, so that higher final conversions and rates of polymerization could be obtained with Py-OXEs. Influence of the OXE structure (both chromophores and leaving groups) is discussed on the basis of different characterization techniques such as: UV-visible absorption spectroscopy, photolysis experiments, real-time Fourier transform infrared spectroscopy (RT-FTIR), stationary fluorescence and time-

resolved fluorescence. Therefore, a global mechanism is finally provided based on the complementary characterization data. Oxime ester derivatives were also tested under air for the generation of 3D patterns (by Direct Laser Write DLW) using a diode laser at 405 nm.

Keywords: Anthracene, Pyrene, Oxime Ester, Free Radical Photopolymerization, Light-Emitting Diodes (LED), 3D printing.

1. Introduction

The synthesis of less energy-intensive materials, with a short preparation time, having good chemical, physical and mechanical properties currently represents a great challenge for industries wishing to manufacture more ecological materials. Hence, chemists have been interested for decades in the development of more environmentally-friendly synthetic routes by introducing light into synthetic processes. Nowadays, Free Radical Photopolymerization (FRP) [1-5] is already present in different areas of our daily life, such as cosmetics [6], dentistry [7], automotive [8], composites [9] and also 3D printing [10].

One drawback of the current approach is the use of UV Hg lamp. UV light is well-known to be harmful for health, by causing skin cancers and eye damages. Parallel to this, the light penetration achievable with UV light is low so that light is unable to penetrate into thick samples. Therefore, these expensive and energy-consuming devices need to be replaced by near-UV and even visible light-emitting diodes (LEDs) [11-17] which are considered as safe irradiation sources, having long operating lifetimes and generating little heat during operation. To make this approach possible, very efficient photoinitiating systems capable of absorbing light must be present into the photocurable resins. Indeed, visible light is less energetic than UV light so that a higher reactivity of the photoinitiating systems has to be found in order to compensate the lower energy of photons. In order to reduce the complexity of the formulations linked to the use of different additives (e.g. co-initiators), mono-component Type I photoinitiators (PIs) are highly desired. These compounds can generate the initiating radicals through a direct homolytic cleavage of a specific bond of the molecule, the cleavage being photochemically induced by mean of the LED light. Their excited states are short-lived (vs. Type II photoinitiator) and hence less quenched by oxygen i.e. Type I

PIs can be preferred for polymerization under air, these photoinitiating systems being less prone to oxygen inhibition.

One of the best classes of Type I PIs known for their reactivity and their effectiveness in initiating radical polymerization are undoubtedly oxime esters (OXEs) [18-23]. Photoinduced homolytic cleavage of the N-O bond is at the origin of the remarkable reactivity of these compounds, which produces iminyl and acyloxy radicals capable of undergoing a decarboxylation reaction (CO_2 release) in charge of reducing the oxygen inhibition by releasing gas within the resin and by limiting oxygen diffusion. Overall, the decarboxylation reaction provides a unique opportunity to increase the reactivity of the developed system.

Recently, research has been conducted on the study of OXEs for Free Radical Photopolymerization [24-28], and these monocomponent systems showed good radical initiation ability under visible light irradiation. Noticeably, absorption properties of oxime esters are governed by the chromophore selected for the design of these Type I photoinitiators. By chemical engineering on the chromophore in charge to interact with light, a good overlap can be obtained between the emission spectra of the LEDs and the absorption spectra of the synthesized OXEs. However, the origin of the excited state associated with the cleavage (S_1 or T_1 state) remains the subject of debates and discussions. Therefore, in this work, two series of oxime esters (Figures 1 and 2) differing by the chromophore were synthesized and developed as Type I photoinitiators for the FRP of acrylates monomers (a benchmark monomer acrylic structure is used here; Figure 3). The first family (17 compounds) contains an anthracene chromophore (An-OXE) and the second family (18 compounds) bears a pyrene group (Py-OXE). Pyrene and anthracene were selected as reference structures reacting mainly from their first excited singlet (S_1) and triplet (T_1) states, respectively. Their fluorescence (Φ_{fluo}) and intersystem crossing (Φ_{isc}) quantum yields are gathered in Table 1. In this work, the effect of the chromophore (pyrene vs. anthracene) on their photochemical properties and photoinitiating abilities will be studied. The proposed PIs (An-OXEs and Py-OXEs) are characterized by good absorption properties in the near-UV and visible range. These PIs were also tested for the generation of 3D polymer patterns by 3D printing experiments.

Table 1. Photophysical parameters characterizing anthracene and pyrene; from [29]

	Φ_{fluo}	Φ_{isc}
Anthracene	0.3	0.71
Pyrene	0.65	0.37

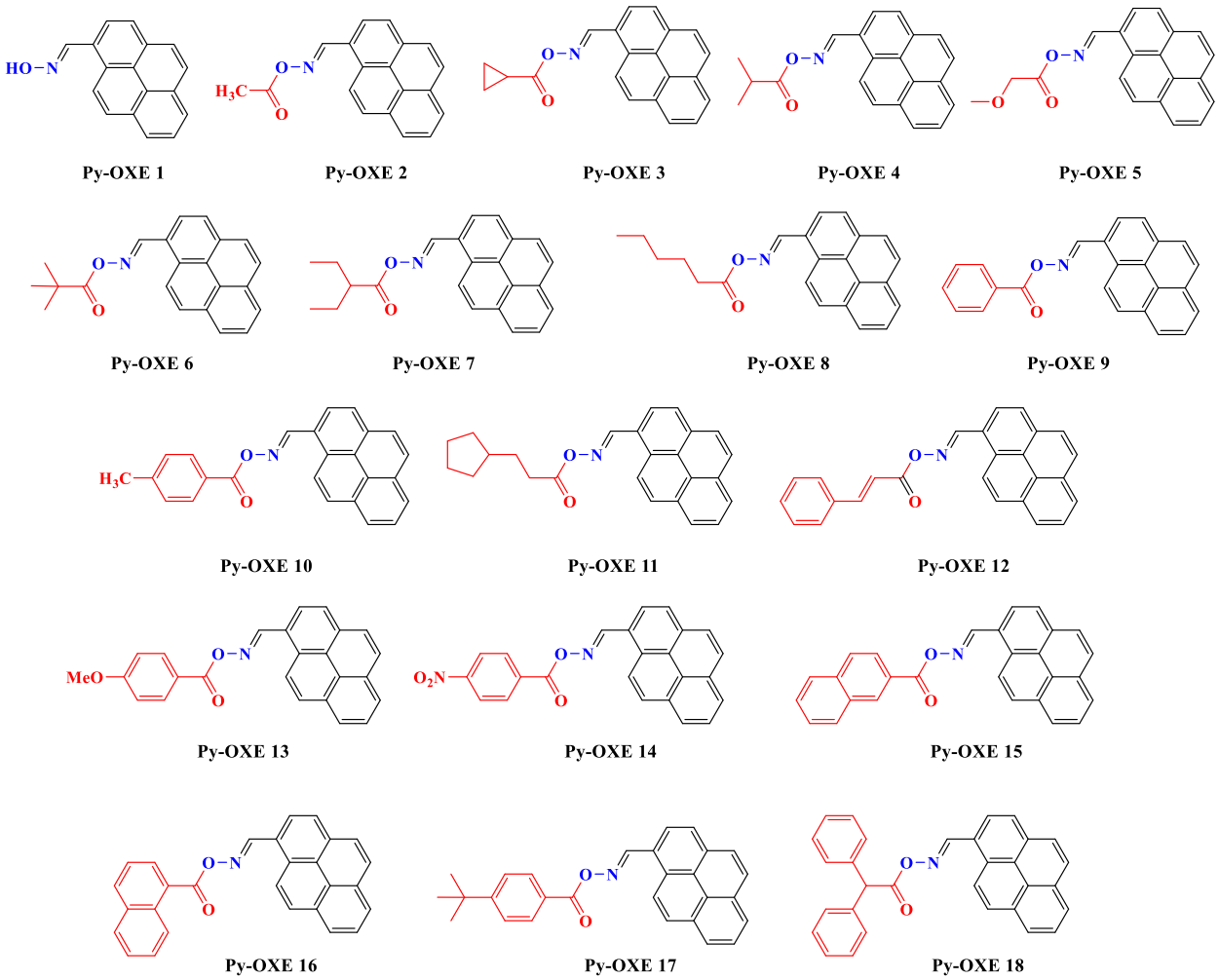

Figure 1. Chemical structures of the Py-OXE investigated in this work.

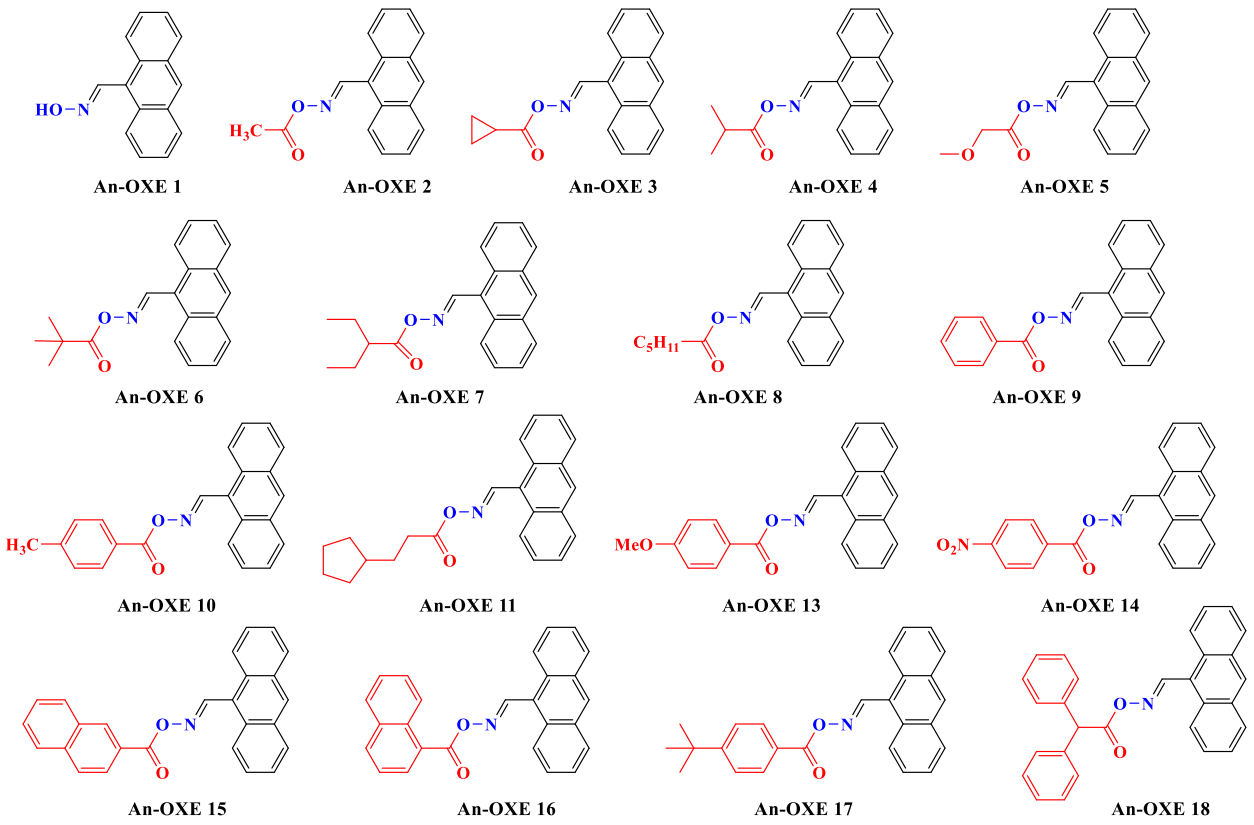

Figure 2. Chemical structures of the An-OXE examined in this work.

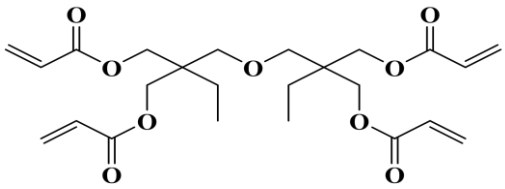

Figure 3. Benchmark acrylate monomer (TA) used in this work.

2. Materials and Methods

2.1 Synthesis of the investigated Oxime-esters/Chemicals

Synthesis of the different oxime esters is described in detail in the results and discussion part and the characterization of the new structures are given in supporting information. Di(trimethylolpropane) tetraacrylate (TA) was provided by Allnex as a benchmark acrylate monomer to investigate the photoinitiating ability of the new proposed PIs.

2.2 Irradiation sources

In this work, a Light-Emitting Diodes (LED) emitting at 405 nm was used as a safe irradiation source for both the photolysis and the photopolymerization experiments (I = 110 mW/cm^2).

2.3 Free Radical Photopolymerization (FRP) characterized by Real-time Fourier Transform Infrared Spectroscopy (RT-FTIR)

In this study, all oxime esters derivatives (An-OXE and Py-OXE) have been used as Type I photoinitiators for the FRP of acrylate functions using TA as the benchmark monomer upon LED @ 405nm illumination. These compounds were used with 0.5% from the global monomer content An-OXE, Py-OXE (0.5% w). In fact, the reactive functions conversion (FC) of FRP process and the polymerization rate (Rp) were monitored by following by evolution of the C=C peak located at 1630 cm^{-1} for the thin samples (25 μm) as presented by us in [7,14-15].

2.4 UV-visible absorption spectra, steady state photolysis, emission spectra, and time-resolved fluorescence spectroscopy experiments

Steady state fluorescence experiments were carried out on a JASCO FP-6200 spectrofluorimeter. Energy of the first singlet excited state E_{S1} was determined from the crossing point of the absorption and emission spectra. Fluorescence lifetime τ_0 for the different dyes were calculated using a time-correlated single-photon counting system (HORIBA® Delta Flex with a HORIBA® PPD-850 as detector) as presented by us in [20].

2.5 Computational Procedure

Molecular orbital calculations were achieved with the Gaussian 09 suite of programs. The Bond Dissociation Energies (BDE (N-O)) and the triplet state energies for the different compounds were investigated at UB3LYP/6-31G* level as presented by us in [20].

2.6 Direct Laser Write (DLW)

3D polymers patterns were obtained by polymerization under air of the photosensitive formulation using a computer-controlled diode laser at 405 nm (spot size = 50 μm), which were

analyzed by a numerical optical microscope (DSX-HRSU from OLYMPUS Corporation). The setup is presented more in detail in [20].

3. Results

3.1 Synthesis of the new Oxime-Esters

All oxime esters investigated in this work were obtained in two steps, starting from the commercially available 9-anthracenecarboxaldehyde or 1-pyrenecarboxaldehyde. In first step, the two oximes could be obtained by reaction of the corresponding aldehyde with hydroxylamine hydrochloride in basic conditions. Especially, a water-soluble base was selected, namely sodium acetate. The reaction was carried out in a mixture of three solvents i.e. methanol, THF and water. The two oximes could be obtained with reaction yields higher than 96%. While investigating the esterification of oximes, surprisingly, while using triethylamine as the base, no esters could be obtained with anthracene-9-carbaldehyde oxime. Instead, a dehydration reaction was observed, furnishing anthracene-9-carbonitrile as the unique reaction product (See Figure 4). Its chemical structure could be unambiguously identified by X-ray diffraction, crystals of this structure being obtained by slow evaporation of chloroform. To get the different anthracene-based oxime esters, mixture of anthracene-9-carbaldehyde oxime with one equivalent of the appropriate acid chloride furnished the targeted oxime esters in high yield. 17 different acid chlorides were used to prepare the different esters, varying from aromatic to aliphatic acid chlorides (See Scheme 1). Diversity of acid chlorides was notably justified by the possibility upon cleavage and decarboxylation reaction of radicals to generate aromatic but also aliphatic primary, secondary and tertiary radicals, stabilized and destabilized radicals. In the case of anthracene-based oxime esters, only the cinnamoyl derivative i.e. **An-OXE 12** could not be obtained, despites several attempts. In the case of pyrene-based oxime esters, the different compounds **Py-OXE 1-Py-OXE 18** could be obtained in classical conditions, by deprotonation of pyrene-1-carbaldehyde oxime with an excess of triethylamine followed by esterification with the appropriate acid chlorides. A summary of the reaction yields is given in the Table 2.

Table 2. Reaction yields obtained during the esterification of the two oximes.

esters	**Py-OXE 1**	**Py-OXE 2**	**Py-OXE 3**	**Py-OXE 4**	**Py-OXE 5**	**Py-OXE 6**	**Py-OXE 7**	**Py-OXE 8**	**Py-OXE 9**
reaction yields (%)	96	86	81	84	83	80	94	91	80
esters	**Py-OXE 10**	**Py-OXE 11**	**Py-OXE 12**	**Py-OXE 13**	**Py-OXE 14**	**Py-OXE 15**	**Py-OXE 16**	**Py-OXE 17**	**Py-OXE 18**
reaction yields (%)	80	83	68	87	93	86	81	83	85
esters	**An-OXE 1**	**An - OXE 2**	**An - OXE 3**	**An - OXE 4**	**An - OXE 5**	**An - OXE 6**	**An - OXE 7**	**An - OXE 8**	**An - OXE 9**
reaction yields (%)	98	78	89	88	82	76	77	88	82
esters	**An - OXE 10**	**An - OXE 11**	**An - OXE 12**	**An - OXE 13**	**An - OXE 14**	**An - OXE 15**	**An - OXE 16**	**An - OXE 17**	**An - OXE 18**
reaction yields (%)	88	84	n.o.[1]	72	86	74	78	88	92

[1] : not obtained.

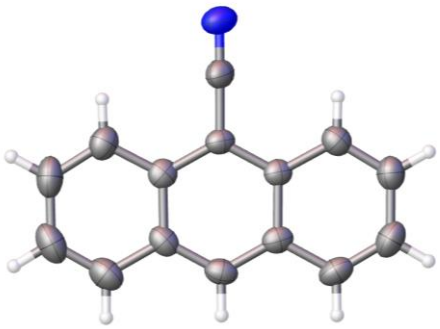

Figure 4. Chemical structure of the side-product formed under basic conditions starting from anthracene-9-carbaldehyde oxime determined by X-ray diffraction.

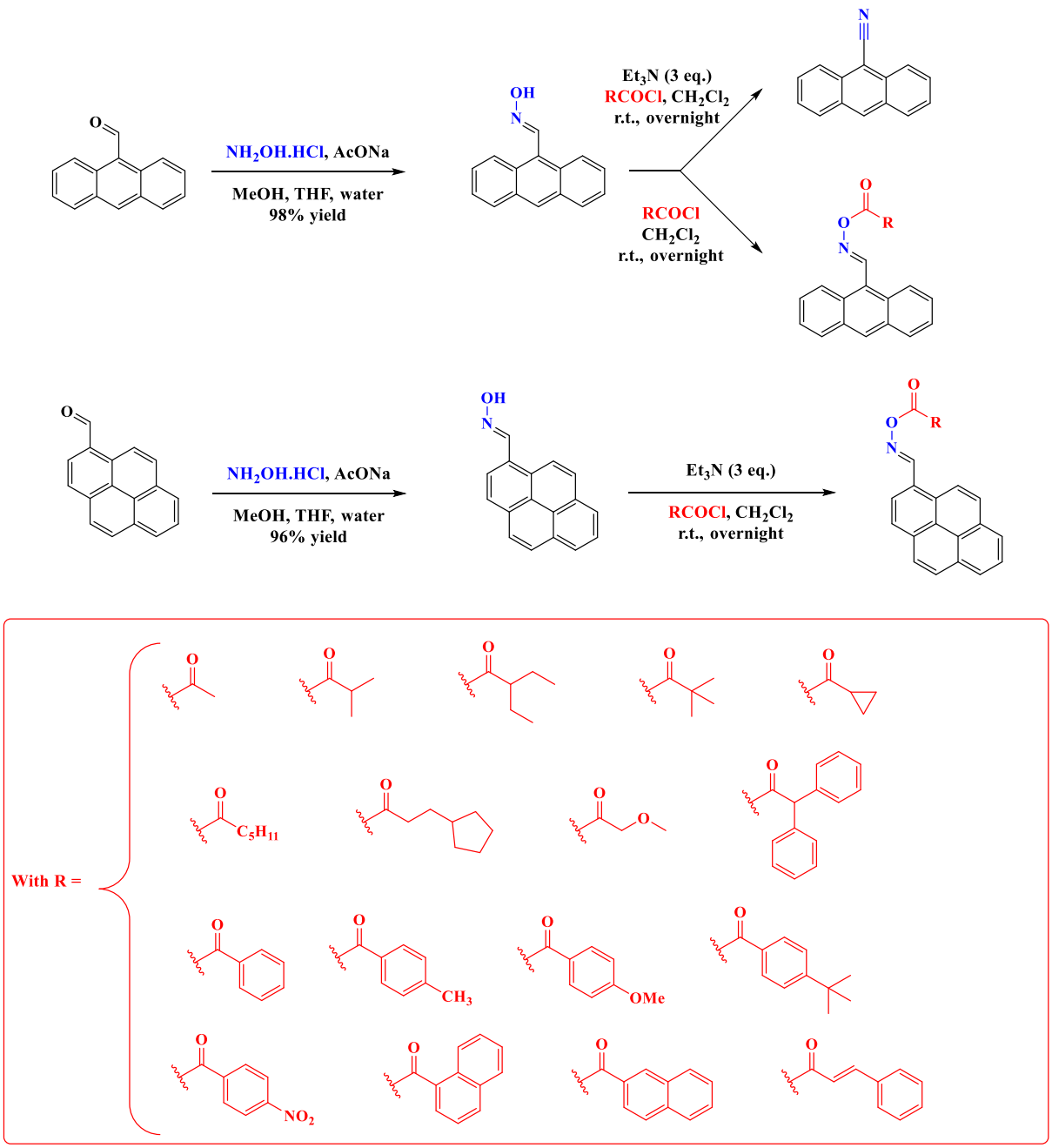

Scheme 1. Synthetic routes to the different anthracene and pyrene-based oxime esters.

3.2 Light absorption properties of Py-OXE

UV-visible absorption spectra of the investigated OXEs bearing a pyrene group were determined in acetonitrile (CAN) and the different curves are presented in Figure 5 (See also Table 3). Comparison with An-OXE will be given below in part 4.2. These organic compounds are

characterized by a wide absorption band and a high ability to absorb the light in the near-UV and visible range between 300-425 nm, e.g. $\varepsilon_{Py\text{-}OXE}$ = 52000 $M^{-1}.cm^{-1}$ at 361 nm for Py-OXE2; 42500 $M^{-1}.cm^{-1}$ at 362 nm for Py-OXE3; 40600 $M^{-1}.cm^{-1}$ at 364 nm for Py-OXE12. In fact, these oxime esters are also characterized by good absorption abilities at 405 nm which ensure a good overlap with the emission spectra of the LEDs used in this work (at 405 nm).

Remarkably, the general shape of the absorption spectra of these compounds is quite similar while the molar extinction coefficients (e.g. at 405 nm) are different e.g. $\varepsilon_{Py\text{-}OXE}$ = 0 $M^{-1}.cm^{-1}$ for Py-OXE1; 1340 $M^{-1}.cm^{-1}$ for Py-OXE2 and 4110 $M^{-1}.cm^{-1}$ for Py-OXE12. These results are related to the different substituents linked to the oxime ester functions for example, a naphthyl (Py-OXE16) group induces an increase of the molar extinction coefficient vs. a methyl group (Py-OXE2).

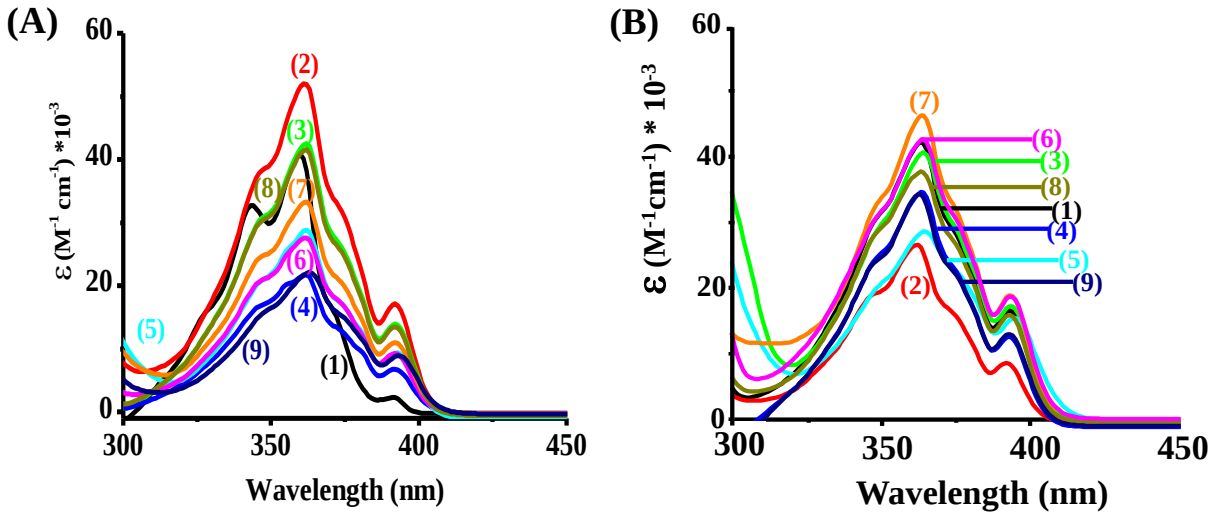

Figure 5. (A) UV-visible absorption spectra of the Py-OXE derivatives in ACN: **(1)** Py-OXE 1, **(2)** Py-OXE 2, **(3)** Py-OXE 3, **(4)** Py-OXE 4, **(5)** Py-OXE 5, **(6)** Py-OXE 6, **(7)** Py-OXE 7, **(8)** Py-OXE 8, **(9)** Py-OXE 9. **(B)** UV-visible absorption spectra of the Py-OXE derivatives in ACN: **(1)** Py-OXE 10, **(2)** Py-OXE 11, **(3)** Py-OXE 12, **(4)** Py-OXE 13, **(5)** Py-OXE 14, **(6)** Py-OXE 15, **(7)** Py-OXE 16, **(8)** Py-OXE 17, **(9)** Py-OXE 18.

Table 3. Absorption properties of Py-OXEs at λ_{max} and 405nm (in acetonitrile (ACN)).

	λ_{max} (nm)	ε_{max} ($M^{-1} cm^{-1}$)	ε_{405nm} ($M^{-1} cm^{-1}$)
Py-OXE1	359	40500	0
Py-OXE2	361	52000	1340
Py-OXE3	362	42500	1160
Py-OXE4	361	21760	580
Py-OXE5	362	28830	535
Py-OXE6	362	27560	770
Py-OXE7	362	33300	1100
Py-OXE8	362	41560	960
Py-OXE9	362	22000	1530
Py-OXE10	362	42190	2620
Py-OXE11	362	26570	545
Py-OXE12	364	40600	4110
Py-OXE13	363	34630	1200
Py-OXE14	362	28640	6400
Py-OXE15	364	42600	4400
Py-OXE16	364	46300	3400
Py-OXE17	363	37720	2720
Py-OXE18	362	34250	1560

3.3 Photopolymerization experiments using TA as benchmark acrylate monomer

3.3.1 Free Radical Photopolymerization using An-OXE PIs

FRP experiments in thin samples were carried out using An-OXEs as Type I photoinitiators (0.5% w/w vs. the monomer content) using TA as the benchmark monomer (See Figure 3). In fact, the different FRP profiles (conversion vs. irradiation time) are shown in Figure 6, and the conversion data are summarized in Table 4. First of all, the different compounds showed more or

less effective polymerization profiles, so that, low final acrylate function conversions (FCs) were observed for the majority of An-OXE upon irradiation at 405nm e.g. FC = 32% for An-OXE2, 50% for An-OXE4, 34% An-OXE6. For TA (without PIs), no polymerization occurs clearly suggesting the Type I initiator behavior of An-OXEs.

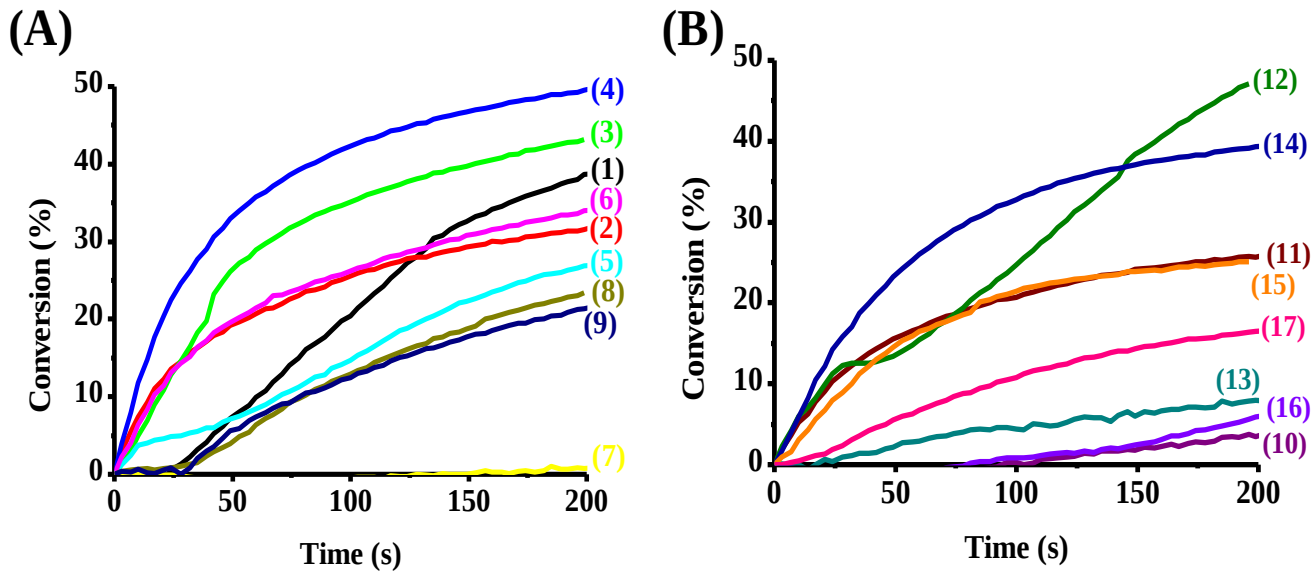

Figure 6. (A), (B) Photopolymerization profiles of acrylates functions using the TA monomer (acrylate function vs. irradiation time) performed in Thin sample in laminate upon irradiation at 405 nm using one-component PISs (0.5%) : **(1)** An-OXE 1, **(2)** An-OXE 2, **(3)** An-OXE 3, **(4)** An-OXE 4, **(5)** An-OXE 5, **(6)** An-OXE 6, **(7)** An-OXE 7, **(8)** An-OXE 8, **(9)** An-OXE 9, **(10)** An-OXE 10, **(11)** An-OXE 11, **(12)** An-OXE 13, **(13)** An-OXE 14, **(14)** An-OXE 15, **(15)** An-OXE 16 **(16)** An-OXE 17, **(17)** An-OXE 18. **Irradiation starts at t = 0 s.**

3.3.2 Free Radical Photopolymerization using Py-OXE PIs

In this part, the anthracene chromophore is now replaced by a pyrene group (Py-OXE). FRP of thin acrylate formulations was carried out in laminate upon irradiation with a LED at 405 nm (I = 110 mW/cm^2). Photopolymerization profiles are now presented in Figure 7 and the conversion data are gathered in Table 4**.** In fact, very interesting results were obtained for the different Py-OXE (0.5% w) systems during the FRP of TA compared to that obtained with the An-OXE analogues, for example, FC = 79% for Py-OXE2; 63% for Py-OXE3; 74% for Py-OXE4; 76% for Py-OXE 7 vs. 32% for An-OXE2; 43% for Py-OXE3; 50% for Py-OXE4. Rates of polymerization were also much higher when working with pyrene derivatives (see the comparison in part 4.2 below). These results clearly show the dramatic impact of pyrene on the polymerization profiles of acrylate functions compared to the anthracene chromophore which only exhibits poor photoinitiation capacity. The results also showed that Py-OXE bearing alkyl substituents on the

ester moieties are more efficient for the polymerization ability e.g. FC = 79% for Py-OXE2 with methyl group, vs. 25% for Py-OXE15 with a naphthyl group.

It is important to note that these oxime esters showed great efficiency compared to the reference structures (Py-OXE1 or An-OXE1) which possess a N-OH group unable to fragment and generate radicals. This clearly shows the interest of the oxime ester functions in the photopolymerization process e.g. FC = 14% for Py-OXE1 vs. 79% Py-OXE2.

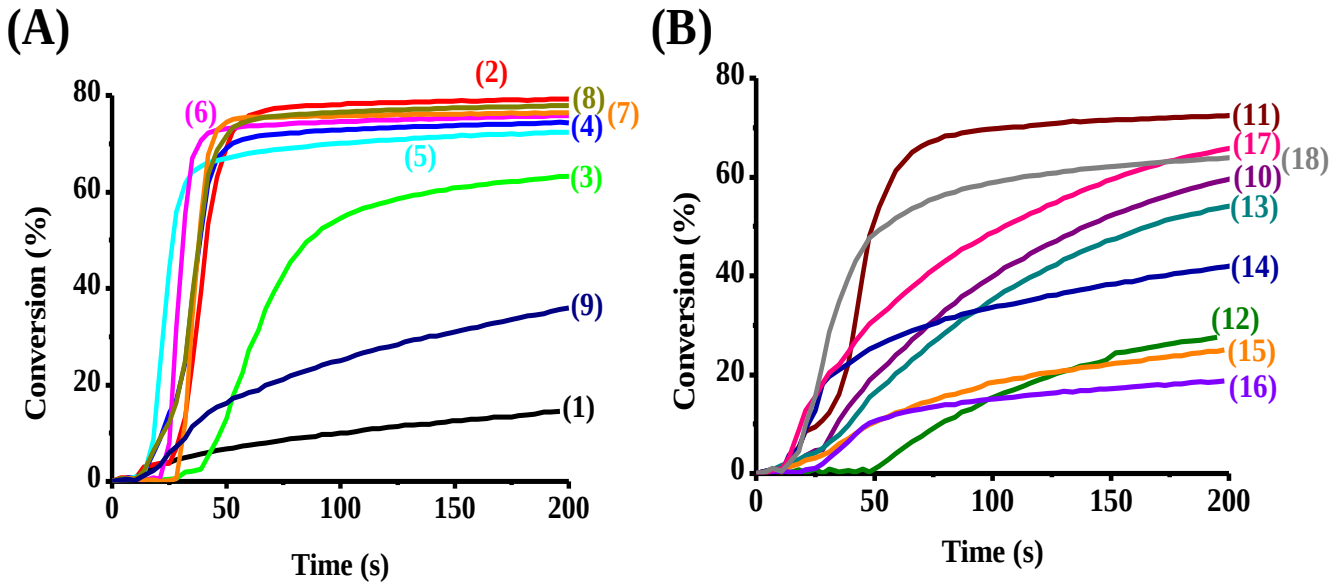

Figure 7. (A), (B) Photopolymerization profiles of acrylates functions using the TA monomer (acrylate function vs. irradiation time) performed in Thin sample in laminate upon irradiation at 405 nm using one-component PISs (0.5%): **(1)** Py-OXE 1, **(2)** Py-OXE 2, **(3)** Py-OXE 3, **(4)** Py-OXE 4, **(5)** Py-OXE 5, **(6)** Py-OXE 6, **(7)** Py-OXE 7, **(8)** Py-OXE 8, **(9)** Py-OXE 9, **(10)** Py-OXE 10, **(11)** Py-OXE 11, **(12)** Py-OXE 12, **(13)** Py-OXE 13, **(14)** Py-OXE 14, **(15)** Py-OXE 15 **(16)** Py-OXE 16, **(17)** Py-OXE 17, **(18)** Py-OXE 18. **Irradiation starts at t = 15 s.**

Table 4. Final reactive (acrylate) function conversions (FC%) for TA using Py-OXEs or An-OXEs upon visible light irradiation using the LED @405 nm.

	Py-OXE	**An-OXE**
OXE-1	14%	39%
OXE-2	79%	32%
OXE-3	63%	43%
OXE-4	74%	50%
OXE-5	72%	27%
OXE-6	76%	34%
OXE-7	76%	23%
OXE-8	78%	0%
OXE-9	36%	22%
OXE-10	60%	0%
OXE-11	72%	26%
OXE-12	28%	-
OXE-13	54%	47%
OXE-14	42%	0%
OXE-15	25%	39%
OXE-16	19%	25%
OXE-17	66%	0%
OXE-18	64%	16%

3.4. Direct laser write using Py-OXEs

To highlight the importance of the pyrene-based oxime esters as Type I photoinitiators for the Free Radical photopolymerization, direct laser write experiments were carried out under air using a laser diode at 405 nm (I = 110 mW/cm²). The generated 3D patterns were characterized by optical numerical microscopy. In fact, Py-OXE were used with 0.5% and they showed a good efficiency in these experiments. A good thickness could also be obtained (~ 2000 μm) with a high spatial resolution. Very short irradiation times were also necessary to generate the 3D patterns. The obtained results are presented in Figure 8.

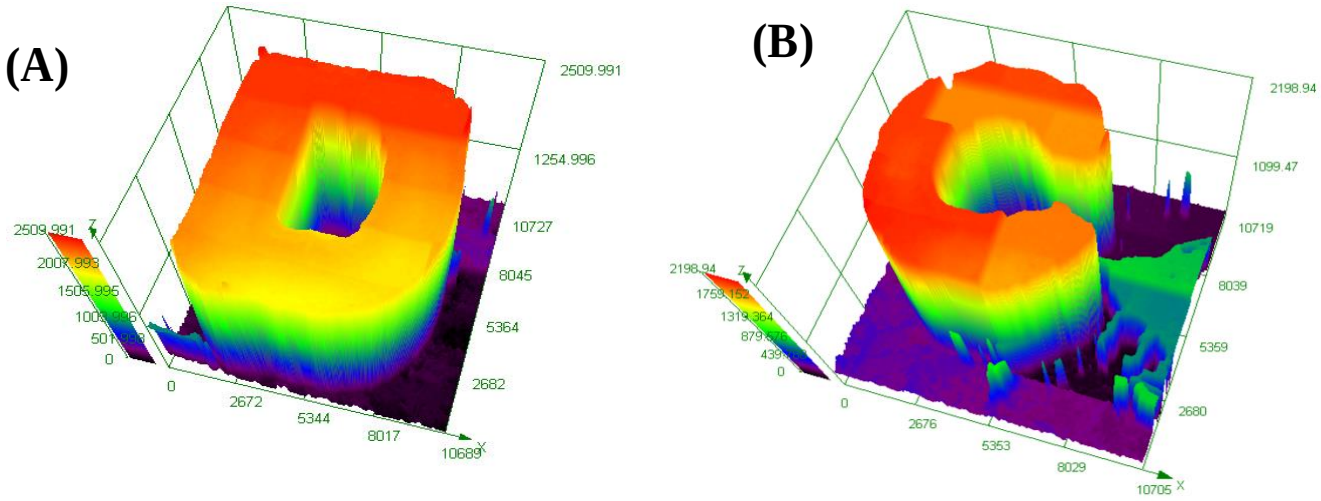

Figure 8. 3D Polymer patterns generated by the FRP process using a diode laser @405 nm characterized by numerical optical microscopy: **(A)** Py-OXE5 (0.5%) and **(B)** Py-OXE8 (0.5 %) in TA.

4. Discussion

Photochemical and photophysical properties as well as the structure/reactivity/efficiency of the investigated oxime esters are now discussed in this part.

4.1 Photochemical mechanisms

Steady state photolysis, excited state lifetimes as well as the emission spectra for the investigated oxime esters (with pyrene and anthracene chromophore) were carried out in ACN using UV-visible absorption spectroscopy, time-resolved and steady state fluorescence spectroscopies, respectively. The results are gathered in Figures 9, 10 and 11.

First, the obtained results showed that a very low decrease on the absorption band of the An-OXEs upon irradiation at 405 nm, in agreement with their poor photosensitivity to be decomposed and produce the reactive species. These results explain the low reactivity of the An-OXE to induce the FRP (See Figure 9).

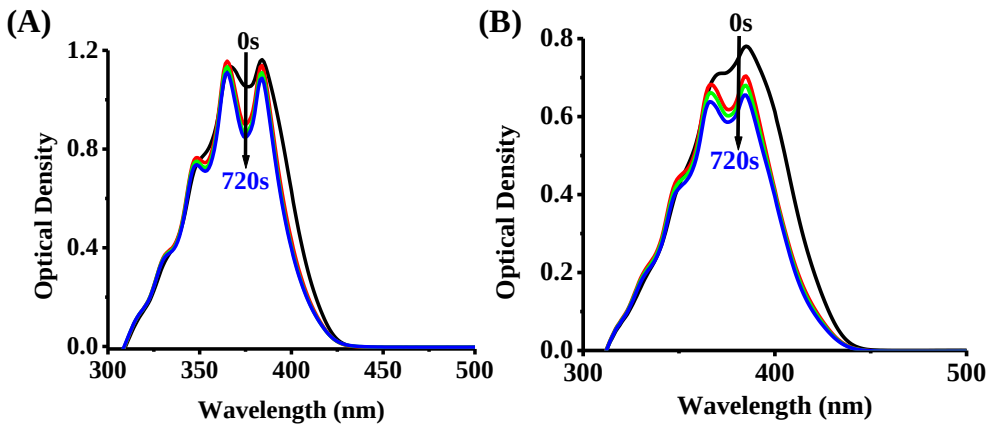

Figure 9. Photolysis experiments of **(A)** An-OXE1 and **(B)** An-OXE 2 at 405nm.

Conversely, a good/excellent photolysis ability was observed for Py-OXE derivatives (See Figure 10) compared to the reference structure (Py-OXE1) or even An-OXEs which showed very low photolysis. These results can be explained by the low N-O bond dissociation energies of the Py-OXE derivatives compared to the reference structure Py-OXE1, e.g., BDE_{N-O} = 61.15 kcal/mol for Py-OXE1 vs. 47.86, 45.65, 47.39, 47.82 kcal/mol for Py-OXE2,3,4,5 respectively (Table 5), and by a high excited state lifetime of Py-OXE1 vs. the ester Py-OXEs (τ_0 = 6.8 ns for Py-OXE1 vs. 3.8, 3.66, 3.8, 3.14 ns for Py-OXE2,3,4,5) which strongly suggest a singlet state cleavage processes (Figure 11 and Table 5).

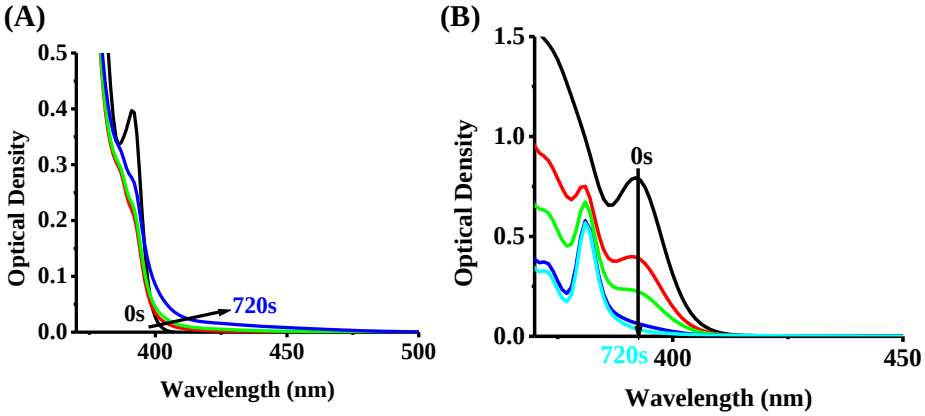

Figure 10. Photolysis experiments of **(A)** Py-OXE1 and **(B)** Py-OXE 2 at 405 nm.

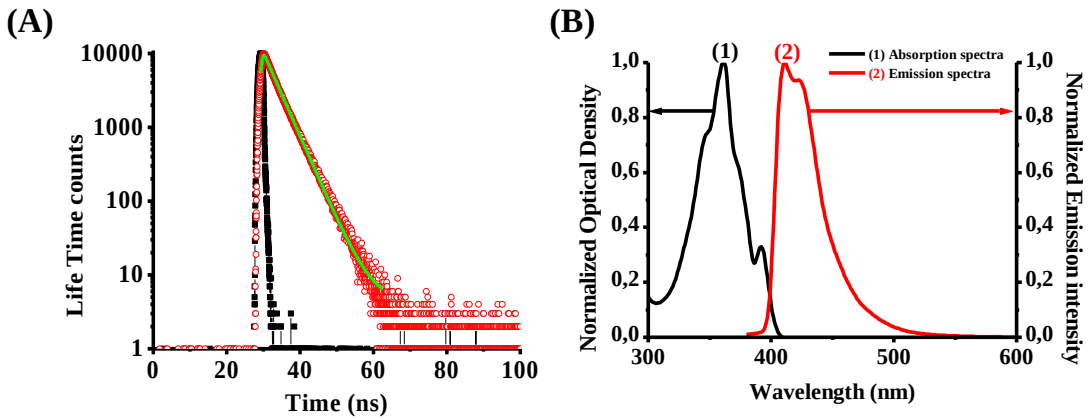

Figure 11. For Py-OXE2 in acetonitrile: **(A)** Excited state lifetime determination, **(B)** E_{S1} determination.

Table 5. Parameters characterizing the An-OXEs and Py-OXEs. Some parameters characterizing the proposed PIs were calculated by molecular modelling: the bond dissociation energy BDE (N–O), the triplet state energy E_{T1}, the singlet excited state energy E_{S1} (evaluated experimentally from the experimental absorption and fluorescence spectra). The S_1 excited state lifetimes were determined by time resolved fluorescence spectroscopy.

PI	BDE_{N-O} (kcal/mol)	E_{S1} (kcal/mol)	τ_0 (S_1) (ns)	E_{T1} (kcal/mol)
1	63.25[a] 61.15[b]	68.95[a] 74.49[b]	4.58[a] 6.8[b]	33.75[a] 41.70[b]
2	44.95[a] 47.86[b]	66.41[a] 71.72[b]	1.5[a] 3.8[b]	39.54[a] 41.56[b]
3	45.74[a] 45.65[b]	n.d	3.66[b]	34.48[a] 41.48[b]
4	44.73[a] 47.39[b]	n.d	3.8[b]	34.08[a] 41.56[b]
5	46.98[a] 47.82[b]	n.d	3.14[b]	34.34[a] 41.39[b]
6	43.78[a] 46.70[b]	n.d	3.75[b]	39.72[a] 41.53[b]
7	43.72[a] 46.84[b]	n.d	3.7[b]	39.55[a] 41.55[b]
8	46.33[a] 46.66[b]	n.d	3.79[b]	34.28[a] 41.40[b]
9	44.48[a] 47.34[b]	n.d	3.02[b]	39.48[a] 41.43[b]
10	46.60[a] 47.17[b]	n.d	2.56[b]	34.47[a] 41.43[b]
11	44.92[a] 47.94[b]	n.d	2.57[b]	39.48[a] 41.57[b]
12	43.65[b]	n.d	n.d	43.45[b]
13	46.29[a] 46.93[b]	n.d	n.d	34.46[a] 41.43[b]

14	46.52 [a] 45.00 [b]	n.d	n.d	39.37 [a] 43.57 [b]
15	44.34 [a] 42.92 [b]	n.d	n.d	39.47 [a] 43.65 [b]
16	45.59 [a] 41.88 [b]	n.d	n.d	34.65 [a] 43.50 [b]
17	46.61 [a] 47.17 [b]	n.d	n.d	34.50[a] 41.43 [b]
18	44.61 [a] 47.65 [b]	n.d	n.d	33.80 [a] 41.56 [b]
a: An-OXE b: Py-OXE n.d: not determined				

Based on these data, a global mechanism can be proposed. First of all, Py-OXEs absorb the light and can be promoted in their excited states (r1) where a cleavage of the N-O bond can undergo, followed by a decarboxylation reaction (r2-r3) in charge of the generation of the initiating radicals (r3).

$$PI\ (h\nu) \rightarrow {}^1PI \qquad r1$$

$${}^1PI \rightarrow R_1R_2C{=}N^{\bullet} + {}^{\bullet}O\text{-}C(=O)\text{-}R_3 \qquad r2$$

$${}^{\bullet}O\text{-}C(=O)\text{-}R_3 \rightarrow R_3^{\bullet} + CO_2 \qquad r3$$

The cleavage from S_1 is found to be energetically favorable (E_{S1} > BDE (N-O)) whereas those from the triplet state are not favorable E_{T1} < BDE (N-O) e.g. for Py-OXE2 (E_{S1} = 71.72 kcal/mol; E_{T1} = 41.56 kcal/mol vs. BDE (N-O) = 47.86 kcal/mol).

4.2 Comparison Anthracene vs. Pyrene derivatives

The effect of the anthracene and pyrene chromophores on the absorption properties as well as the initiation ability of the FRP are compared in Figures 6 and 7 and Table 4**.** The obtained results showed a high initiating capacity of the oxime esters bearing a pyrene chromophore compared to those comprising an anthracene group (FC = 32% for An-OXE2 vs. 79% for Py-OXE2). Markedly, despite the anthracene-based oxime-esters absorb more light at 405 nm compared to the pyrene oxime esters (ε = 4000 vs. 1580 $M^{-1}cm^{-1}$ for An-OXE 2 and Py-OXE 2 respectively), the pyrene derivatives are more reactive in agreement with their better cleavage ability (See Figure 12). This

latter behavior can be ascribed to the cleavage ability from S_1 (see above); the intersystem crossing being favorable for anthracene derivatives (see the chromophore properties in Table 1).

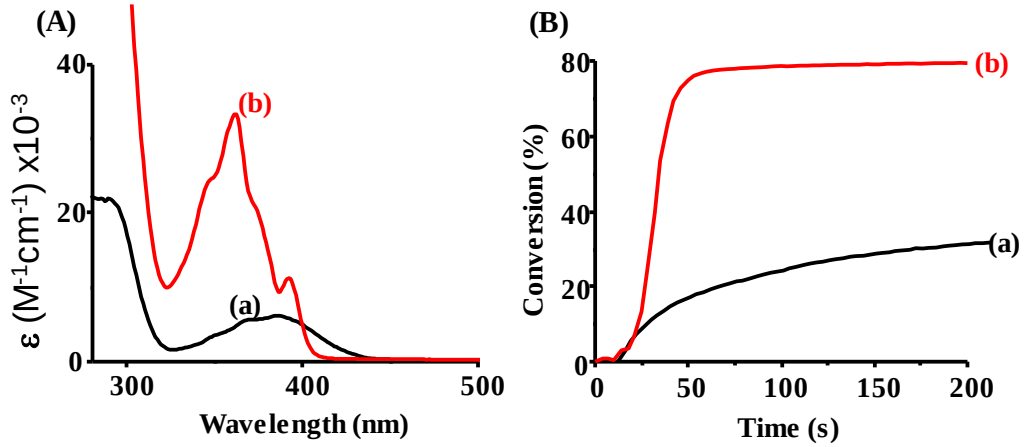

Figure 12. **(A)** UV-visible absorption spectra of **(a)** An-OXE 2 and **(b)** Py-OXE 2. **(B)** Photopolymerization profiles of acrylates functions using **(a)** An-OXE 2 (0.5% w) and **(b)** Py-OXE 2 (0.5% w) as photoinitiators.

5. Conclusion

In this work, two series based on Pyrene-OXE and Anthracene-OXE were synthesized and developed as Type I photoinitiators for the free radical photopolymerization of acrylate monomer (e.g. TA) under visible light irradiation at 405 nm. The FRP results were explained and discussed using different characterization techniques: steady state photolysis, time-resolved fluorescence spectroscopy, fluorescence spectroscopy and molecular modeling. The obtained results showed a very good initiation ability of the new investigated oxime esters, in particular, those bearing a pyrene group, which allows their use in direct laser write experiments where they produce polymers with high spatial resolution. This work paves the way for the development of new visible light absorbing Type I photoinitiators.

Acknowledgments

The authors thank Aix Marseille University and the Centre National de la Recherche Scientifique for financial support.

References

1. Fouassier, J.P.; Morlet-Savary, F.; Lalevée, J.; Allonas, X.; Ley, C. Materials **2010**, 3, 5130.

2. Fouassier, J.P.; Lalevée, J. Photoinitiators for polymer synthesis: Scope, Reactivity, and efficiency. Wiley-VCH Verlag GmbH &Co.KGaA: Weinheim, Germany, **2012**.

3. Fouassier, J.P. Photopolymerization and Photo-curing: Fundamentals and Applications. Gardner Publications: New York,NY, USA, **1995**.

4. Dietliker, K.A. Compilation of Photoinitiators Commercially Available for UV Today. Sita Technology Ltd.: Edinbergh, London, **2002**.

5. Davidson, S. Exploring the Science, Technology and Application of UV and EB Curing. Sita Technology Ltd.: Edinbergh, London, **1999**.

6. Morgan, S.E.; Havelka, K.O.; Lochhead, R.Y. Cosmetic Nanotechnology: Polymers and Colloids in Cosmetics in Person Care. ACS Symposium Series: Washington, DC, USA, **2007**.

7. Bouzrati-Zerelli, M.; Maier, M.; Dietlin, C.; Morlet-Savary, F.; Fouassier, J.P.; Klee, J.E.; Lalevée, J. Dental Mater. **2016**,32, 1226.

8. Garcès, J.M.; Moll, D.J.; Bicerano, J.; Fibiger, R.; McLeod, D.G. Adv.Mater. **2000**, 12, 1835.

9. Garra, P.; Bonardi, A.H.; Baralle, A.; Al Mousawi, A.; Bonardi, F.; Dietlin, C.; Morlet- Savary, F.; Fouassier, J.P.; Lalevée, J. Polym.Sci. Part A: Polym. Chem. **2018**, 56, 889.

10. Lawrence, J.R.; O'Neill, F.T.; Sheridan, J.T. **2001**, 112, 449.

11. Fouassier, J.P.; Lalevée, J. Photochemistry. **2014**, 42, 215.

12. Dumur, F.; Gigmes, D.; Fouassier, J.-P.; Lalevée, J. Acc. Chem. Res. **2016**, 49, 1980.

13. Dietlin, C.; Schweizer, S.; Xiao, P.; Zhang, J.; Morlet-Savary, F.; Graff, B.; Fouassier, J.P.; Lalevée, J. Polym. Chem. **2015**, 6, 3895.

14. Zivic, N.; Bouzrati-Zerelli, M.; Kermagoret, A.; Dumur, F.; Fouassier, J.P.; Gigmes, D.; Lalevée, J. Chem. Cat. Chem. **2016**, 8, 1617.

15. Dietlin, C.; Schweizer, S.; Xiao, P.; Zhang, J.; Morlet-savary, F.; Graff, B.; Fouassier, J.P.; and Lalevée, J. Polym. Chem. **2015**, 6, 3895.

16. Schmitt, M.; Lalevée, J. Colloids Surf. A, **2017**, 532, 189.

17. Schmitt, M. RSC Adv. **2015**, 52, 67284.

18. Qiu, W.; Li, M.; Yang, Y.; Li, Z.; Dietliker, K.; Polym. Chem. **2020**, 11, 1356.

19. Zhou, R.; Sun, X.; Mhanna, R.; Malval, J.P.; Jin, M.; Pan, H.; Wan, D.; Morlet-Savary, F.; Chaumeil, H.; Joyeux, C. Series. ACS Appl. Polym. Mater. **2020**, 5, 2077.

20. Lee, Z. H.; Hammoud, F.; Hijazi, A.; Graff, B.; Lalevée, J.; Chen, Y.C. Polym. Chem. **2021**, 12, 1286.

21. Fast, D.E.; Lauer, A.; Menzel, J.P.; Kelterer, A.M.; Gescheidt, G.; Barner-Kowollik, C. Macromolecules **2017**, 50, 1815.

22. Groenenboom, C.J.; Hageman, H.J.; Oosterhoff, P.; Overeem, T.; Verbeek, J. Photochem. Photobiol. A: Chem. **1997**, 107, 261.

23. Chen, S.; Jin, M.; Malval, J.P.; Fu, J.; Morlet-Savary, F.; Pan, H.; Wan, D. Polym. Chem. **2019**, 48, 6609.

24. Wang, W.; Jin, M.; Pan, H.; Wan, D. Prog.Org.Coat. 2021, 151, 106019.

25. Han, W.; Shi, Y.; Xue, T.; Wang, T. Dyes Pigm. **2019**, 166, 140.

26. Ma, X.Y.; Cao, D.; Fu, H.Y.; You, J.; Gu, R.Q.; Fan, B.F.; Nie, J.; Wang, T. Prog. Org. Coat. **2019**, 135, 517.

27. Ma, X.Y.; Gu, R.Q.; Yu, L.J.; Han, W.X.; Li, J.; Li, X.Y.; Wang, T. Polym. Chem. **2017**, 8, 6134.

28. Qiu, W.W.; Hu, P.; Zhu, J.Z.; Liu, R.; Li, Z.Q.; Hu, Z.Y.; Chen, Q.D.; Dietliker, K.; Liska, R. ChemPhotoChem **2019**, 3, 1090.

29. Handbook of photochemistry, Third edition, Montalti, M.; Credi,A.; Prodi, L.; Gandolfi, M.T. CRC Press, 2006, Boca Raton, FL.

TOC graphic: